

# Sensing hydrogen peroxide using a glassy carbon electrode modified with in-situ electrodeposited platinum-gold bimetallic nanoclusters on a graphene surface

Xiu Cui · Shengnan Wu · Yongxin Li · Gang (Gary) Wan

Received: 2 April 2014 / Accepted: 1 July 2014 / Published online: 22 July 2014  
© Springer-Verlag Wien 2014

**Abstract** Platinum-gold nanoclusters (PtAu NCs) were electrodeposited on graphene placed on the surface of a glassy carbon electrode (GCE). The PtAu-graphene nanocomposite was characterized by X-ray diffraction, transmission electron microscopy, scanning electron microscopy, and electrochemical methods. The PtAu NCs display excellent electrocatalytic activity towards the reduction of hydrogen peroxide. This effect was exploited in a sensor that responds (at a working voltage of 100 mV) to H<sub>2</sub>O<sub>2</sub> in the 15 nM to 8.73 μM concentration range, with a limit of detection at 8.0 nM.

**Keywords** PtAu bimetallic nanoclusters · Graphene · Hydrogen peroxide · Electrochemical sensor

## Introduction

Recently, bimetallic alloys have received extensive attentions because their properties often differ markedly from either of the constituent metals, with the mixtures frequently exhibiting enhanced catalytic stability, activity or selectivity, which makes them widely be used in catalysis and sensing fields [1–5]. Au-Pt bimetallic nanoparticles have been widely reported for catalytic applications, and it has been found that the morphologies of

them can affect their catalytic activities, which are different from their individual nanoparticles. Now Au-Pt alloy is widely used as a catalyst in fuel cells [6–8], oxygen reduction reaction [4] or sensors applications [3, 9, 10].

To maximize the electrocatalytic activity of Au-Pt nanoparticles, some suitable carbon substrates [11, 12], such as carbon black and carbon nanotubes, are always used as a support to disperse these nanoparticles. Owing to its extraordinary electronic transport properties, huge surface area and excellent catalytic activity, Graphene, a single-atom-thick sheet of hexagonally arrayed sp<sup>2</sup>-bonded carbon atoms, has been extensively investigated in physics, chemistry, and material science, which makes it be considered as a promising candidate as a novel 2D substrate to load Pt, Au, and Pd nanoparticles for the applications in catalysis, energy and sensing [11–13].

Hydrogen peroxide is one of the most important analytes nowadays due to its extensive existence in food, environment, and biological bodies, which is also involved in many biological events and intracellular pathways [14]. Many electrochemical methodologies have been developed to detect hydrogen peroxide [14–19]. Herein, we present a facile approach to synthesize Au-Pt bimetallic nanoclusters uniformly dispersed on graphene surface by in-situ electrodeposition method, which has been used to fabricate hydrogen peroxide sensor. Electrocatalytic result shows that the Au-Pt bimetallic nanoclusters have excellent electrocatalytic activity towards the reduction of hydrogen peroxide, which can be used to fabricate hydrogen peroxide sensor with high sensitivity.

X. Cui · S. Wu · Y. Li (✉)  
College of Chemistry and Materials Science, Anhui Normal University, Wuhu 241000, China  
e-mail: yongli@mail.ahnu.edu.cn

Y. Li  
e-mail: yongxin.li@coe.montana.edu

Y. Li  
Corrosion and Sustainable Infrastructure Lab, Western Transportation Institute, Montana State University, PO Box 174250, Bozeman, MT 59717-4250, USA

G. Wan  
Texas A&M University Libraries, College station, TX 77845, USA

## Experimental

### Materials and reagents

Hydrogen tetrachloroaurate hydrate (HAuCl<sub>4</sub>·4H<sub>2</sub>O, 99.9 %), Hexachloroplatinic (IV) acid (H<sub>2</sub>PtCl<sub>6</sub>·6H<sub>2</sub>O, 99.9 %),

hydrogen peroxide ( $\text{H}_2\text{O}_2$ ) were obtained from Sinopharm Group Chemical Reagent Co. (Shanghai, China. [www.sinopharmholding.com/](http://www.sinopharmholding.com/)). Graphene was the product of Nanjing first abundance nanomaterials technology company (Nanjing, China. <http://www.ecvv.com/>), which was synthesized from graphene oxide (GO) firstly [20, 21], and then was prepared by the chemical reduction of GO with hydrazine [22], which was denoted as RGO. The TEM image of RGO was given as Fig. 1a, which shows that RGO sheets are rippled and entangled with each other due to the thermodynamic stability of the 2D membrane.

All chemical and reagents were of analytical grade and used without further purification. All of the solutions were prepared with doubly distilled water.

## Apparatus

Electrochemical experiments, including cyclic voltammetry (CV), Chronoamperometry and electrochemical impedance spectroscopy (EIS), were performed on a CHI 660C electrochemical workstation (ChenHua, Shanghai, China. [http://chi.](http://chi.instrument.com.cn)

[www.rigaku.com](http://www.rigaku.com)). The diffraction patterns were recorded using a Rigaku Dmax-B X-ray diffractometer (Tokyo, Japan. <http://www.rigaku.com>). FE-SEM images were made on a Hitachi S-4800 field-emission scanning electron microscope operated at an accelerating voltage of 5.0 kV (Tokyo, Japan. [www.hitachi-hita.com/](http://www.hitachi-hita.com/)).

All experiments were carried out with a three-electrode system consisting of an Ag/AgCl reference electrode, a Pt foil auxiliary electrode and a glass carbon disk electrode (GCE,  $\Phi$  3.0 mm) electrode as a working electrode. A digital pH/mV meter (model 780 Metrohm, Jiangsu, China) was applied for the measurement of pH to prepare phosphate buffered solution. Electrochemical impedance spectroscopy (EIS) measurements were carried out in 10 mM  $\text{K}_3[\text{Fe}(\text{CN})_6]$  :  $\text{K}_4[\text{Fe}(\text{CN})_6]$  (1:1) mixture containing 0.1 M KCl. All the experiments were at room temperature.

## Fabrication of PtAu/RGO/GCE Electrode

Prior to modification, GCE was polished before each experiment with 1.0, 0.3, and 0.05  $\mu\text{m}$  alumina powders in sequence, rinsed with double-distilled water, and sonicated in

**Fig. 1** (a) The TEM image of RGO. (b) Typical SEM image of Au–Pt nanoclusters deposited on RGO/GCE. Inset: SEM image of single Au–Pt nanoparticle selected from b. (c) Typical XRD patterns of PtAu nanoclusters deposited on RGO/GCE. (d) Cyclic voltammogram of the Au–Pt nanoclusters modified on RGO/GCE in 0.5 M  $\text{H}_2\text{SO}_4$  under air at a scan rate of  $50 \text{ mV} \cdot \text{s}^{-1}$

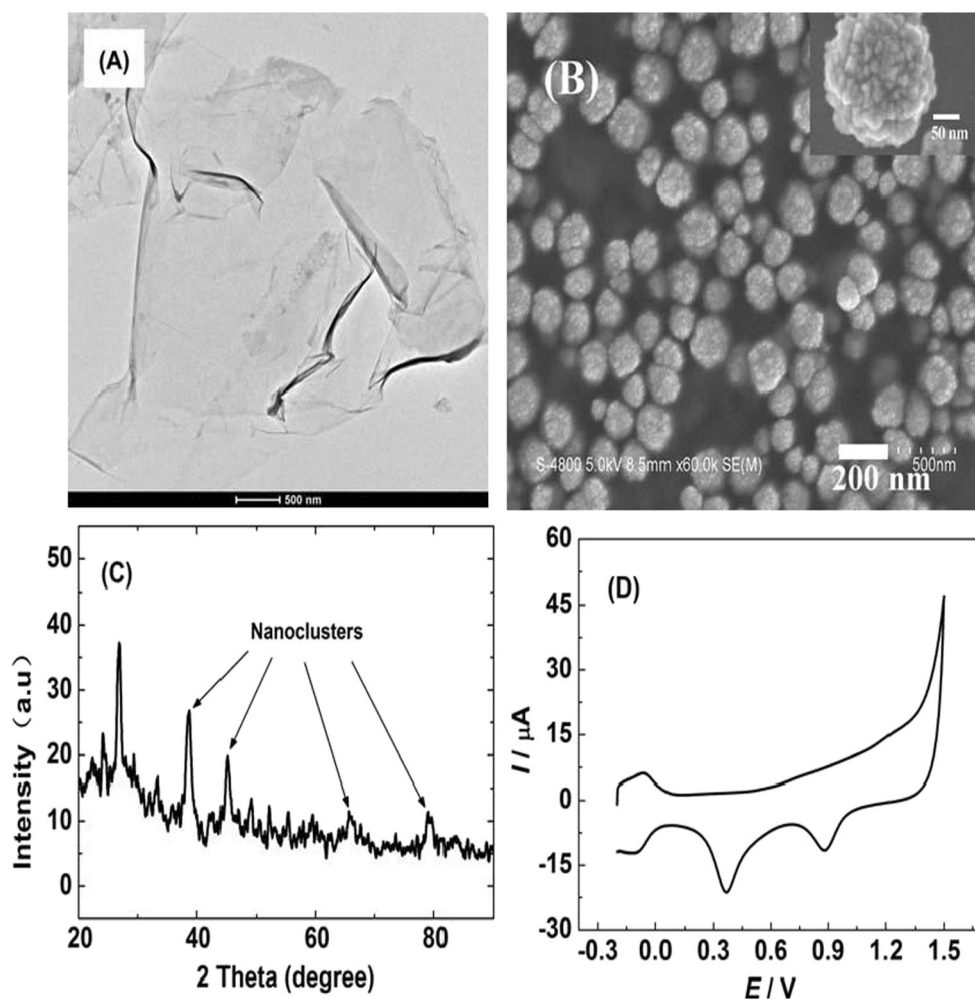
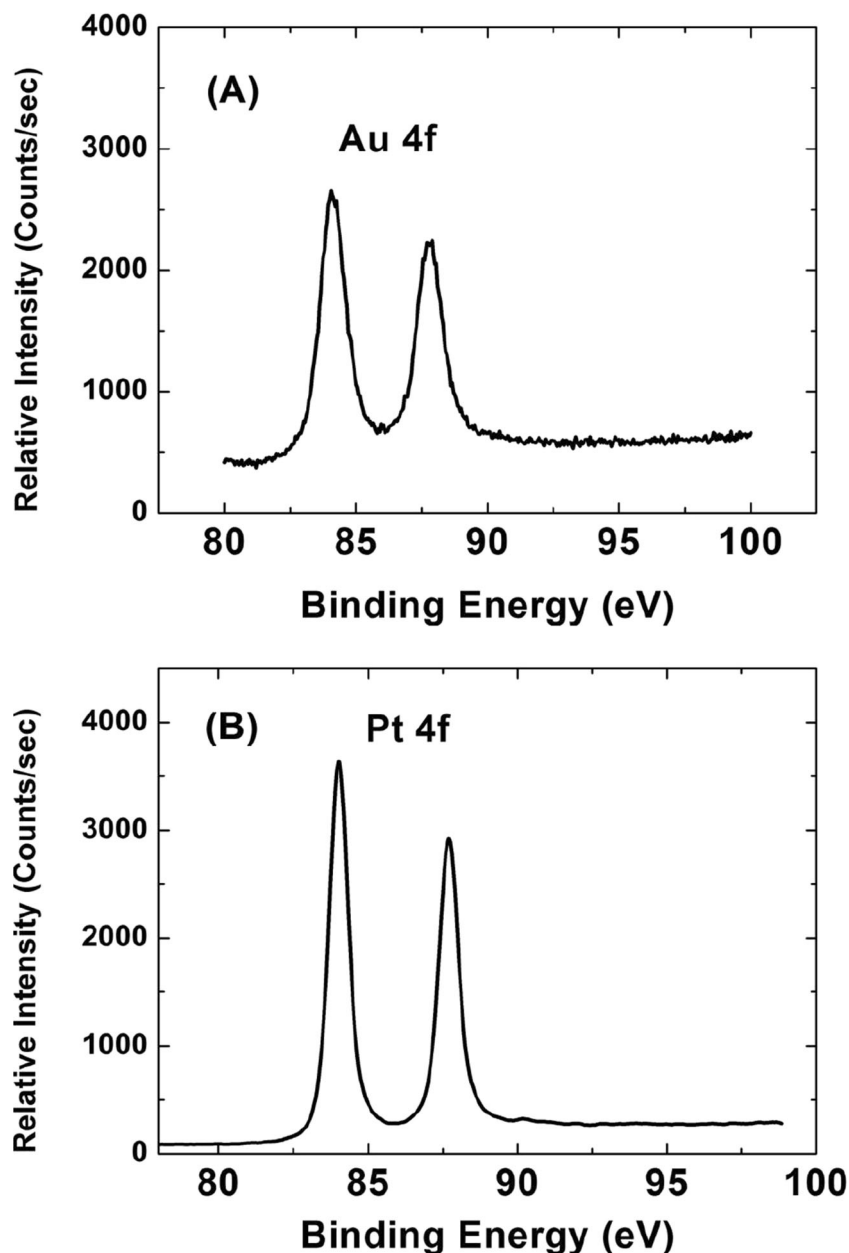


**Fig. 2** XPS spectra of PtAu NCs on electrode surface



ethanol and double-distilled water for 5 min, respectively. The polished electrode was dried with a high purity nitrogen stream immediately before use.

The RGO (1 mg) sheets were first dispersed into distilled water (1 mL) to form a black homogeneous suspension ( $1 \text{ mg} \cdot \text{mL}^{-1}$ ). Then the suspension ( $6 \mu\text{L}$ ) was cast onto the surface of GCE with a micro-syringe, and the solvent was evaporated at ambient temperature before use. At last, the RGO will form a thin film on the GCE surface through  $\pi$ - $\pi$  electronic interaction between graphene and GCE, which was denoted as RGO/GCE.

The electrochemical deposition of PtAu nanoclusters was performed in  $0.20 \text{ M H}_2\text{SO}_4$  aqueous solution containing

$0.5 \text{ mM HAuCl}_4$  and  $0.5 \text{ mM H}_2\text{PtCl}_6$ . The deposition time was 400 s, and the deposition potential was selected as  $-0.2 \text{ V}$ .

## Results and discussion

### Characterization of the PtAu/graphene nanocomposites

The morphology of PtAu nanoclusters modified on the graphene/GCE surface was characterized by FE-SEM, as shown in Fig. 1b, it could be seen that the PtAu nanoclusters with average diameter  $\sim 200 \text{ nm}$  were consisted of small nanoparticles. We have reported that Pt nanoclusters can be formed

on choline modified GCE due to the special function of choline through the progressive nucleation process, but no clusters structures can be found on bare GCE surface [23]. During the process, the seed nucleation was slow and new nuclei continuously formed, which resulted in the formation of nanostructures consisting of many small nanoparticles. Herein, it can be deduced that the growth of PtAu bimetallic nanoclusters is also through the progressive nucleation mechanism. The nanoclusters were not observed for direct electro-deposition on the bare GCE surface (data now shown), indicating that the graphene layer could affect the growth of bimetallic nanoclusters. In the electrodeposition process, the solution of 0.2 M  $\text{H}_2\text{SO}_4$  was used as the supporting electrolyte, which made graphene layer had a very open structure, and more metallic ions could be adsorbed on the graphene surface and reduced to metallic nanoparticles. Previous results [5, 24, 25] showed that the graphene layer modified on the surface could lead to the formation of novel gold or Pd aggregates by electrodeposition. Therefore, the graphene layer could also affect the morphologies of PtAu nanostructures though the detailed mechanism requires further investigation.

The crystalline structure of the Pt-Au nanoclusters was characterized by XRD measurements. The XRD pattern of the nanoclusters was provided in Fig. 1c. The peaks at  $2\theta = 38.7^\circ$ ,  $45.2^\circ$ ,  $65.9^\circ$ , and  $78.8^\circ$  were from the bimetallic nanoclusters, which can be assigned to PtAu(111),  $-(200)$ ,  $-(220)$ , and  $-(311)$ , clearly demonstrating that PtAu NCs have a face-centered cubic (fcc) structure. The peak at  $26.3^\circ$  was from the graphene layer. The average size of the deposited nanoparticles was calculated to be about 12 nm based on the Scherrer formula [23, 26]. It was known that the positions ( $2\theta$ ) of the peaks of deposited pure gold nanoparticles were  $38.2^\circ$ ,  $44.4^\circ$ ,  $65.1^\circ$  and  $76.2^\circ$ , and platinum nanoparticles were  $39.8^\circ$ ,  $46.1^\circ$ ,  $67.7^\circ$  and  $81.8^\circ$ , respectively, corresponding to the face-centered cubic crystal structure were observed [23]. The peaks of bimetallic nanoflowers lay in between those of pure gold and platinum nanoparticles, indicating that the

deposited nanoclusters were not the mixtures of individual nanoparticles but bimetallic nanostructures [27].

XPS measurements were also performed to identify the PtAu NCs on a glassy carbon chip, and high resolution scans of the Au 4f and Pt 4f regions are shown in Fig. 2. The Au 4f<sub>7/2</sub> peak is located at a binding energy of 84.0 eV, which corresponds to zero-valent Au [28]. The Pt 4f<sub>7/2</sub> peak is located at a binding energy of 71.2 eV, which corresponds to zero-valent Pt [28].

To further characterize the properties of the PtAu bimetallic nanoclusters, the cyclic voltammogram (CV) of the bimetallic nanoclusters modified graphene/GCE in 0.5 M  $\text{H}_2\text{SO}_4$  have been recorded at a scan rate of  $50 \text{ mV s}^{-1}$  from  $-0.2$  to  $1.5 \text{ V}$  (Fig. 1d). The peaks appeared at about  $-0.12 \text{ V}$  correspond to the hydrogen adsorption and desorption. The platinum oxide reduced at about  $0.33 \text{ V}$  was also observed. The Au oxidation and reduction peaks also appeared between  $0.87$  and  $1.35 \text{ V}$ . The electrochemical properties of nanoclusters deposited on the electrode surface were similar to those of bare gold and platinum electrodes, indicating that the deposited nanoclusters consisted of bimetallic nanoparticles.

EIS is an effective method for probing the features of a surface-modified electrode using the redox probe,  $\text{Fe}(\text{CN})_6^{3-}/\text{Fe}(\text{CN})_6^{4-}$  [29, 30]. Fig. 3a illustrates the results of impedance spectroscopy on the bare GCE (curve a), RGO/GCE (curve b), Pt/GCE (curve c) PtAu/GCE (curve d) and PtAu/RGO/GCE (curve e) in the presence of equivalent 10 mM  $\text{Fe}(\text{CN})_6^{3-/4-}$ . The electro-transfer resistance ( $R_{\text{et}}$ ) value can be directly measured as the semicircle diameter. As shown in Fig. 3a, the  $R_{\text{et}}$  value for the modified electrode is decreased dramatically in comparison with bare GCE, which should be ascribed to the good properties of PtAu nanoclusters and graphene layer that formed a high electron conduction pathway between the electrode surface and the  $\text{Fe}(\text{CN})_6^{3-}/\text{Fe}(\text{CN})_6^{4-}$  probe. This result has also indicated that the PtAu nanoclusters and graphene layer are gradually immobilized on the surface of the GCE.

The CVs have been employed to investigate the electrochemical properties of modified electrode. As shown in

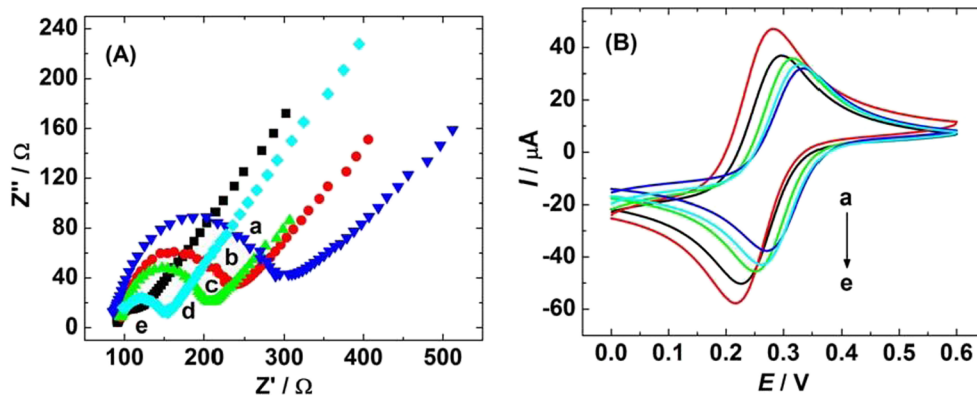


**Fig. 3** **A** Complex plane impedance plots in 10 mM  $\text{K}_3[\text{Fe}(\text{CN})_6]:\text{K}_4[\text{Fe}(\text{CN})_6]$  (1:1) mixture containing 0.1 M KCl at the bare GCE (a), RGO/GCE (b), Pt/GCE (c), PtAu/GCE (d) and

PtAu/RGO/GCE (e). **B** CVs of 5.0 mM  $\text{K}_3[\text{Fe}(\text{CN})_6]+0.1 \text{ M KCl}$  at bare GCE (a), RGO/GCE (b), Pt/GCE (c), PtAu/GCE (d) and PtAu/RGO/GCE (e). Scan rate:  $50 \text{ mV s}^{-1}$



Fig. 3b, a pair of quasi-reversible redox peaks of  $\text{Fe}(\text{CN})_6^{3-}$  with a peak separation ( $\Delta E_p$ ) of 50 mV exists at the bare GCE (**curve a**). The peak currents increased slightly with RGO/GCE (**curve b**), Pt/GCE (**curve c**), PtAu/GCE (**curve d**) and PtAu/RGO/GCE (**curve e**) due to either the good conductivity of the graphene layer or the large surface area of the metal nanostructures modified on the electrodes surface. These results are in agreement with the EIS data, indicating that the graphene and PtAu nanoclusters have been immobilized on the GCE surface successfully.

Electrochemical performance of the PtAu/RGO/GCE towards the  $\text{H}_2\text{O}_2$  sensing

Figure 4a shows the typical CVs of 0.05 mM hydrogen peroxide at different electrodes. No response is observed for 0.05 mM  $\text{H}_2\text{O}_2$  on bare GCE (**curve a**) and RGO/GCE (**curve b**), and Pt/RGO/GCE gives a very weak response to  $\text{H}_2\text{O}_2$  at a negative potential ( $\sim -0.05$  V, **curve c**), which is similar to

previous report [31]. Although bulk PtAu/GCE exhibits a more sensitive response (**curve d**), the PtAu/RGO/GCE exhibits an excellent response signal, and the peak potential is  $\sim 0.12$  V (**curve e**). Compared with bulk PtAu/GCE, it can be deduced that the excellent electrocatalytic activity towards the reduction of  $\text{H}_2\text{O}_2$  from the PtAu/RGO/GCE is due to the graphene supported PtAu nanoclusters structure, which has larger surface area and good conductivity, and the result is in accordance with previous results [32].

Considering the good electrocatalytic activity of PtAu nanoclusters modified RGO/GCE towards the reduction of  $\text{H}_2\text{O}_2$ , amperometric method for the detection of  $\text{H}_2\text{O}_2$  was attempted. Figure 4b shows the steady-state current responses of the RGO/GCE (**curve a**), Pt/RGO/GCE (**curve b**), Au/RGO/GCE (**curve c**) and PtAu/RGO/GCE (**curve d**), respectively, for the successive additions of certain concentrations of  $\text{H}_2\text{O}_2$  into stirred phosphate buffered solution (pH 7.0) at an applied potential of 0.09 V. As expected from Fig. 4b, the PtAu nanoclusters modified RGO/GCE exhibits much larger catalytic currents in

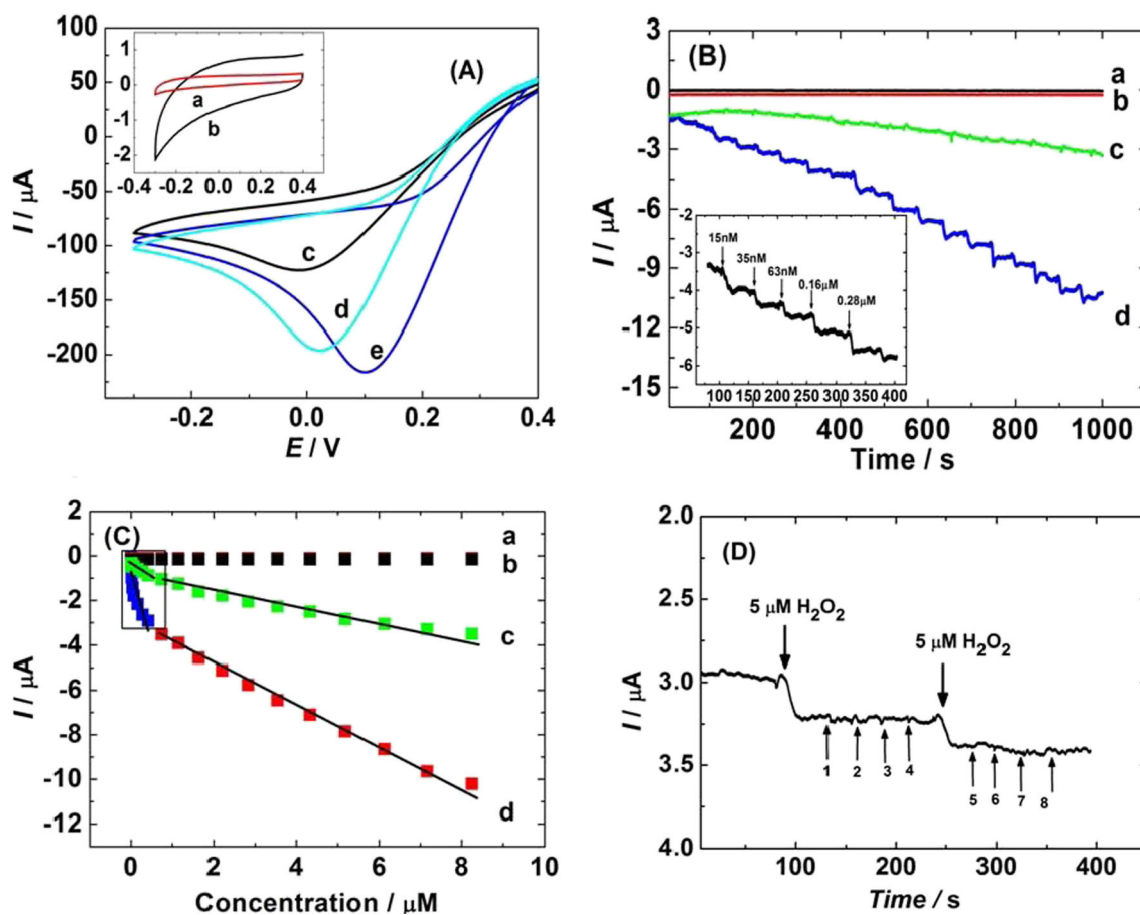


**Fig. 4** **A** CV responses of bare GCE (**a**), RGO/GCE (**b**), Pt/GCE (**c**), PtAu/GCE (**d**) and PtAu/RGO/GCE (**e**) in 1/15 M phosphate buffered solution (pH=7) containing 1 mM  $\text{H}_2\text{O}_2$ , **B** The chronoamperometry responses at applied potential of 0.1 V with injection of various concentrations  $\text{H}_2\text{O}_2$  into 5 mL of stirring phosphate buffered solution at pH 7.0 RGO/GCE (**a**), Pt/GCE (**b**), PtAu/GCE (**c**) and PtAu/RGO/GCE (**d**), respectively. **C** Plots of chronoamperometric currents vs  $\text{H}_2\text{O}_2$

concentration for RGO/GCE (**a**), Pt/GCE (**b**), PtAu/GCE (**c**) and PtAu/RGO/GCE (**d**), respectively. **D** Amperometric response of PtAu/RGO/GCE biosensor upon the detection of 5  $\mu\text{M}$   $\text{H}_2\text{O}_2$  in the presence of the 0.2 mM L-leucine (1), L-phenylalanine (2), L-glutamate (3), L-alanine (4), AA (5), glucose (6), acetic acid (7) and ethanol (8). Inset of **B**: Inset: enlarged  $i-t$  signals between 60 and 400 s. scan rate: 50  $\text{mV}\cdot\text{s}^{-1}$

response to the changes of  $\text{H}_2\text{O}_2$  concentration than that from other modified GCEs. Figure 4c shows the calibration curve of  $\text{H}_2\text{O}_2$  at the PtAu nanoclusters modified RGO/GCE (**curve d**). For comparison, the calibration curves of  $\text{H}_2\text{O}_2$  at the RGO/GCE (**curve a**), Pt/RGO/GCE (**curve b**) and Au/RGO/GCE (**curve c**) are also provided. From Fig. 4c, it can be seen that the calibration curve of  $\text{H}_2\text{O}_2$  at the PtAu nanoclusters modified RGO/GCE is much steeper than that at the other electrodes, indicating there has the highest sensitivity for  $\text{H}_2\text{O}_2$  sensing at the PtAu nanoclusters modified RGO/GCE. From **curve d** in Fig. 4c, It can be seen that at relative low concentration (from 0.015  $\mu\text{M}$  to 0.65  $\mu\text{M}$ , the linear regression equation is  $I(\mu\text{A}) = -6.217 - 4.105 C(\mu\text{M})$  and  $R^2 = 9912$ ), and the calibration plot is steeper than that at high concentration (from 0.82  $\mu\text{M}$  to 8.73  $\mu\text{M}$ , the linear regression equation is  $I(\mu\text{A}) = -17.228 - 0.616 C(\mu\text{M})$  and  $R^2 = 9964$ ), indicating that the PtAu nanoclusters modified RGO/GCE is more sensitive to  $\text{H}_2\text{O}_2$  at low concentration. The detection limit of the  $\text{H}_2\text{O}_2$  was to be 0.008  $\mu\text{M}$  on a signal-to-noise ratio of 3. The response time of the PtAu nanoclusters modified RGO/GCE towards  $\text{H}_2\text{O}_2$  reduction is less than 5 s, validating the rapid catalytic reduction process occurring at the composite film surface. The result illustrates the detection limit is much better than most of  $\text{H}_2\text{O}_2$  sensors, including the usage of graphene as supporting materials [18, 19, 33–39], which are listed in Table 1.

#### Selectivity, stability and reproducibility

For evaluation of the selectivity of the PtAu nanoclusters modified RGO/GCE, some possible interferents were

investigated for their effect on the amperometric detection of  $\text{H}_2\text{O}_2$ . Figure 3d was the amperometric response obtained by the successive additions of 5  $\mu\text{M}$   $\text{H}_2\text{O}_2$  and some possible interferents in phosphate buffered solution at an applied potential of 0.12 V. As shown in Fig. 3d, the responses current of L-leucine, L-phenylalanine, L-glutamate, L-alanine, ascorbic acid (AA), glucose, acetic acid and Ethanol do not cause any observable interference to the detection of  $\text{H}_2\text{O}_2$ . This result suggests that these species had no obvious interference in the detection of  $\text{H}_2\text{O}_2$  and the PtAu nanoclusters modified RGO/GCE has good selectivity towards the reduction of  $\text{H}_2\text{O}_2$ .

The reproducibility of the PtAu nanoclusters modified RGO/GCE was also investigated by measuring the current signal for 10  $\mu\text{M}$   $\text{H}_2\text{O}_2$  at ten modified electrodes at the same condition. The relative standard deviation (RSD) for these ten time measurements was 4.25 %, suggesting the good reproducibility of the prepared electrode. The stability of the biosensor was studied by amperometric measurements in the presence of 5  $\mu\text{M}$   $\text{H}_2\text{O}_2$  periodically. When not in use, the sensor was stored under high humidity (relative humidity, RH >90 %) at 25 °C. After the modified electrode was stored in refrigerator for 10 days, the current response remained 94.1 % of its original response, indicating that the sensor has excellent long-term stability.

#### Conclusions

In this work, AuPt bimetallic NCs were successfully synthesized on RGO/GCE surface by using an in-situ

**Table 1** The comparison of detection limit and linear range from different electrochemical sensors for the determination of  $\text{H}_2\text{O}_2$

Electrodes	Detection limit ( $\mu\text{M}$ )	Linear range ( $\mu\text{M}$ )	References
PB/nanopore <sup>a</sup>	0.6	3.0–210	[18]
AuNPs/ITO <sup>b</sup>	0.01	30–1000	[19]
PB/NPGF <sup>c</sup>	0.36	1.0–100	[33]
GaHCF <sub>6</sub> -CILPE <sup>d</sup>	1.0	–	[34]
CdO/MWCNT/GCE <sup>e</sup>	0.1	0.5–200	[35]
Ag@AgCl nanoboxes/GCE <sup>f</sup>	1.7	5–15000	[36]
GNPs/Graphene/CS/GCE <sup>g</sup>	1.6	5–35000	[37]
DNA-AgNCs/graphene/GCE <sup>h</sup>	3.0	15–25000	[38]
RGO/ZnO/GCE <sup>i</sup>	0.02	0.02–22.48	[39]
PtAu/RGO/GCE	0.008	0.82–8.73	This work

<sup>a</sup> Prussian blue (PB) modified nanopore electrode

<sup>b</sup> gold nanoparticles modified indium tin oxide electrode

<sup>c</sup> Prussian blue (PB) modified nanoporous gold film (NPGF) electrode

<sup>d</sup> Gallium hexacyanoferrate modified carbon ionic liquid paste electrode

<sup>e</sup> cadmium oxide nanoparticles/multiwall carbon nanotube modified glassy carbon electrode

<sup>f</sup> Ag@AgCl nanoboxes modified glassy carbon electrode

<sup>g</sup> gold nanoparticles-graphene-chitosan modified glassy carbon electrode

<sup>h</sup> polynucleotide-templated silver nanoclusters (DNA-AgNCs)/graphene composite modified glassy carbon electrode

<sup>i</sup> reduced graphene oxide (RGO)/zinc oxide (ZnO) composite modified glassy carbon electrode

electrodeposition method. The PtAu NCs-RGO modified GCE as a nonenzymatic sensor exhibited an excellent electrocatalytic activity towards the reduction of  $\text{H}_2\text{O}_2$ . The electrochemical experiments showed that the sensor had high sensitivity, good selectivity and reproducibility, and the PtAu bimetallic NCs-RGO nanocomposites might be used as an effective material for the construction of nonenzymatic amperometric  $\text{H}_2\text{O}_2$  sensor in the future.

**Acknowledgments** This work is financially supported by the National Natural Science Foundation of China (No. 21375002), the Key Project of Chinese Ministry of Education, and Anhui Normal University.

## References

- Hamm G, Becker C, Henry CR (2006) Bimetallic Pd-Au nanocluster arrays grown on nanostructured alumina templates. *Nanotechnology* 17:1943
- Wen D, Guo SJ, Wang YZ, Dong SJ (2010) Bifunctional nanocatalyst of bimetallic nanoparticle/TiO<sub>2</sub> with enhanced performance in electrochemical and photoelectrochemical applications. *Langmuir* 26:11401
- Xiao F, Zhao FQ, Mei DP, Mo ZR, Zeng BZ (2009) Nonenzymatic glucose sensor based on ultrasonic-electrode position of bimetallic PtM (M = Ru, Pd and Au) nanoparticles on carbon nanotubes-ionic liquid composite film. *Biosens Bioelectron* 24:3481
- Peng Z, Yang H (2009) Synthesis and oxygen reduction electrocatalytic property of Pt-on-Pd bimetallic heteronanostructures. *J Am Chem Soc* 131:7542
- Ge S, Yan M, Lu J, Zhang M, Yu F, Yu J et al (2012) Electrochemical biosensor based on graphene oxide-Au nanoclusters composites for L-cysteine analysis. *Biosens Bioelectron* 31:49
- Shang N, Papakonstantinou P, Wang P, Ravi S, Silva P (2010) Platinum integrated graphene for methanol fuel cells. *J Phys Chem C* 114:15837
- Qiu J-D, Wang G-C, Liang R-P, Xia X-H, Yu H-W (2011) Controllable deposition of platinum nanoparticles on graphene as an electrocatalyst for direct methanol fuel cells. *J Phys Chem C* 115:15639
- Luo Z, Yuwen L, Bao B, Tian J, Zhu X, Weng L et al (2012) One-pot, low-temperature synthesis of branched platinum nanowires/reduced graphene oxide (BPtNW/RGO) hybrids for fuel cells. *J Mater Chem* 22:7791
- Chen KJ, Lee CF, Rick J, Wang SH, Liu CC, Hwang BJ (2012) Fabrication and application of amperometric glucose biosensor based on a novel PtPd bimetallic nanoparticle decorated multi-walled carbon nanotube catalyst. *Biosens Bioelectron* 33:75
- Shi HY, Zhang ZX, Wang Y, Zhu QY, Song WB (2011) Bimetallic nano-structured glucose sensing electrode composed of copper atoms deposited on gold nanoparticles. *Microchim Acta* 173:85
- Dong L, Gari RRS, Li Z, Craig MM, Hou S (2010) Graphene-supported platinum and platinum-ruthenium nanoparticles with high electrocatalytic activity for methanol and ethanol oxidation. *Carbon* 48:781
- Bong S, Kim Y-R, Kim I, Woo S, Uhm S, Lee J et al (2010) Graphene supported electrocatalysts for methanol oxidation. *Electrochem Commun* 12:129
- Guo S, Dong S, Wang E (2010) Three-dimensional pt-on-pd bimetallic nanodendrites supported on graphene nanosheet: facile synthesis and used as an advanced nanoelectrocatalyst for methanol oxidation. *ACS Nano* 4:547
- Chen S, Yuan R, Chai Y, Hu F (2013) Electrochemical sensing of hydrogen peroxide using metal nanoparticles: a review. *Microchim Acta* 180:15
- Li S-J, Du J-M, Zhang J-P, Zhang M-J, Chen J (2014) A glassy carbon electrode modified with a film composed of cobalt oxide nanoparticles and graphene for electrochemical sensing of H<sub>2</sub>O<sub>2</sub>. *Microchim Acta* 181:631
- Chen X, Wu G, Cai Z, Oyama M, Chen X (2014) Advances in enzyme-free electrochemical sensors for hydrogen peroxide, glucose, and uric acid. *Microchim Acta* 181:689
- Ren L, Dong J, Cheng X, Xu J, Hu P (2013) Hydrogen peroxide biosensor based on direct electrochemistry of hemoglobin immobilized on gold nanoparticles in a hierarchically porous zeolite. *Microchim Acta* 180:1333
- Doroftei F, Pinteala T, Arvinte A (2014) Enhanced stability of a Prussian blue/sol-gel composite for electrochemical determination of hydrogen peroxide. *Microchim Acta* 181:111
- Xiong W, Qu Q, Liu S (2014) Self-assembly of ultra-small gold nanoparticles on an indium tin oxide electrode for the enzyme-free detection of hydrogen peroxide. *Microchim Acta* 1
- Hummers WS, Offeman RE (1958) Preparation of graphitic oxide. *J Am Chem Soc* 80:1339
- Kovtyukhova NI, Ollivier PJ, Martin BR, Mallouk TE, Chizhik SA, Buzaneva EV et al (1999) Layer-by-layer assembly of ultrathin composite films from micron-sized graphite oxide sheets and polycations. *Chem Mater* 11:771
- Li D, Mueller MB, Gilje S, Kaner RB, Wallace GG (2008) Processable aqueous dispersions of graphene nanosheets. *Nat Nanotechnol* 3:101
- Lin X, Li Y (2006) A sensitive determination of estrogens with a Pt nano-clusters/multi-walled carbon nanotubes modified glassy carbon electrode. *Biosens Bioelectron* 22:253
- Zhang D, Choy WCH, Wang CCD, Li X, Fan L, Wang K (2011) Polymer solar cells with gold nanoclusters decorated multi-layer graphene as transparent electrode. *Appl Phys Lett* 99:223302
- Giorgi L, Giorgi R, Gagliardi S, Serra E, Alvisi M, Signore MA et al (2011) Platinum-gold nanoclusters as catalyst for direct methanol fuel cells. *J Nanosci Nanotechnol* 11:8804
- Radmilovic V, Gasteiger HA, Ross PN (1995) Structure and chemical composition of a supported Pt-Ru electrocatalyst for methanol oxidation. *J Catal* 154:98
- Qian L, Yang XR (2006) Polyamidoamine dendrimers-assisted electrodeposition of gold-platinum bimetallic nanoflowers. *J Phys Chem B* 110:16672
- NIST X-ray Photoelectron Spectroscopy Database. In; 2003.
- Li YX, Wu SN, Chen YL, Lu QF, Wang L (2011) Formation of Au nanoflowers on cysteamine monolayer and their electrocatalytic oxidation of nitrite. *Anal Methods* 3:1399
- Li YX, Xian HY, Zhou Y (2011) Formation of platinum nanoflowers on 3-aminopropyltriethoxysilane monolayer: Growth mechanism and electrocatalysis. *Appl Catal a-Gen* 401:226
- Shen JH, Yang XL, Zhu YH, Kang HG, Cao HM, Li CZ (2012) Gold-coated silica-fiber hybrid materials for application in a novel hydrogen peroxide biosensor. *Biosens Bioelectron* 34:132
- Kristian N, Yan Y, Wang X (2008) Highly efficient submonolayer Pt-decorated Au nano-catalysts for formic acid oxidation. *Chem Commun* 353
- Ghaderi S, Mehrgardi MA (2014) Prussian blue-modified nanoporous gold film electrode for amperometric determination of hydrogen peroxide. *Bioelectrochemistry* 98:64
- Haghighi B, Khosravi M, Barati A (2014) Fabrication of gallium hexacyanoferrate modified carbon ionic liquid paste electrode for sensitive determination of hydrogen peroxide and glucose. *Mater Sci Eng C* 40:204
- Butwong N, Zhou L, Ng-eontae W, Burakham R, Moore E, Srijaranai S et al (2014) A sensitive nonenzymatic hydrogen peroxide sensor

- using cadmium oxide nanoparticles/multiwall carbon nanotube modified glassy carbon electrode. *J Electroanal Chem* 717–718:41
36. Li Y, Zheng J, Sheng Q, Wang B (2014) Synthesis of Ag@AgCl nanoboxes, and their application to electrochemical sensing of hydrogen peroxide at very low potential. *Microchimica Acta* 1.
37. Jia N, Huang B, Chen L, Tan L, Yao S (2014) A simple non-enzymatic hydrogen peroxide sensor using gold nanoparticles-graphene-chitosan modified electrode. *Sensors Actuators B Chem* 195:165
38. Xia Y, Li W, Wang M, Nie Z, Deng C, Yao S (2013) A sensitive enzymeless sensor for hydrogen peroxide based on the polynucleotide-templated silver nanoclusters/graphene modified electrode. *Talanta* 107:55
39. Palanisamy S, Chen S-M, Sarawathi R (2012) A novel non-enzymatic hydrogen peroxide sensor based on reduced graphene oxide/ZnO composite modified electrode. *Sensors Actuators B Chem* 166–167:372